THE ASTROPHYSICAL JOURNAL, 421:115–121, 1994 January 20

A NEAR-INFRARED SPECTROSCOPIC STUDY OF THE LUMINOUS MERGER NGC 3256. II. EVIDENCE FOR FLUORESCENT MOLECULAR HYDROGEN EMISSION

RENÉ DOYON
Département de Physique, Université de Montréal and Observatoire du Mont Mégantic, C.P. 6128, Succ. A., Montréal, Quebec, Canada H3C 3J7
G. S. WRIGHT
Joint Astronomy Centre, 665 Komohana Street, Hilo, HI 96720
AND
R. D. JOSEPH
University of Hawaii, Institute for Astronomy, 2680 Woodlawn Drive, Honolulu, HI 96822
Received 1993 February 22; accepted 1993 August 2

ABSTRACT

The excitation mechanism and origin of the molecular hydrogen (H_2) observed in the starburst galaxy NGC 3256 is discussed. The relative intensities of *K*-window H_2 transitions suggest that roughly half of the 1–0 *S*(1) flux measured on the nucleus is fluorescently excited by UV photons. From a simple geometrical representation of the interstellar medium, in which molecular clouds are bathed in a diffuse UV radiation field, we show that there are enough OB stars and molecular material in the center of the galaxy to reproduce at least half if not all of the observed 1–0 *S*(1) flux. This implies that UV fluorescence is responsible for more than 90% of the total H_2 emission emitted at all wavelengths.

The potential contribution of shock-excited H_2 emission is also investigated. A starburst model is used to predict the time evolution of the 1–0 *S*(1)/Brγ ratio expected from an ensemble of star-forming regions in which the H_2 flux is contributed only by young stellar (Orion-type) objects and supernova remnants. The model can reproduce line ratios in the range of 0.5–1.0, as typically observed in starburst galaxies, provided that the starburst event is older than $\sim$30 million years and the star formation rate is exponentially decreasing. The predictions of the model are valid only for a single-event starburst. Given the age of the burst inferred for NGC 3256 and the observed 1–0 *S*(1)/Brγ ratio, we conclude that less than 30% of the total 1–0 *S*(1) is contributed by young stellar objects and supernova remnants in this galaxy. These results show that the production of both shock- and fluorescently excited H_2 emission in comparable quantities is a natural consequence of starburst activity.

Subject headings: galaxies: individual (NGC 3256) — galaxies: interactions — galaxies: ISM — galaxies: starburst

1. INTRODUCTION

In Paper I (Doyon, Joseph, & Wright 1993, hereafter DJW), we presented and analyzed near-infrared spectra of the merging galaxy NGC 3256. We showed that this galaxy experiences a vigorous episode of star formation activity (starburst). The paper focused on the modeling of the observational properties of the galaxy. We showed how the observations combined with starburst models can be used to obtain quantitative information on the age of the burst and the parameters of the initial mass function (IMF). We also reported the detection of molecular hydrogen emission. The purpose of this second paper is to discuss the origin and the excitation mechanisms responsible for this emission.

The detection of H_2 emission in NGC 3256 is not very surprising since this is a common feature of starburst galaxies. Indeed, H_2 lines have been detected in more than 50 galaxies, among them interacting and merging systems (e.g., Joseph, Wright, & Wade 1984; Rieke et al. 1985; DePoy, Becklin, & Wynn-Williams 1986; Lester, Harvey, & Carr 1988; Prestwich 1989), Seyferts (Thompson et al. 1978; Hall et al. 1981; Fischer et al. 1987; Kawara, Nishida, & Gregory 1987), and bright spirals (Puxley, Hawarden, & Mountain 1988). However, except for a few objects, the nature of the exciting source responsible for the H_2 emission is still unknown.

In general, the H_2 gas can be excited either by collisions or by absorption of ultraviolet (UV) ohotons in the Lyman and Werner electronic bands (912–1108 Å), followed by a deexcitation cascade to the ground state (fluorescence). In principle, both mechanisms can be discriminated by measuring the 2–1 *S*(1)/1–0 *S*(1) and 1–0 *S*(0)/1–0 *S*(1) line ratios which are predicted to be 0.1 and 0.2 in thermal spectra (Hollenbach & Shull 1977; Brand et al. 1988) but as high as 0.5 and 0.6 in the fluorescent case (Black & Dalgarno 1976; Black & van Dishoeck 1987). Collisionally excited H_2 emission has been observed in a variety of galactic sources including young stellar objects (YSOs) or bipolar outflows (e.g., the Orion nebulae; Gautier et al. 1976), planetary nebulae (Treffers et al. 1976), Herbig-Haro objects (Elias 1980), supernova remnants (SNR) (Graham, Wright, & Longmore 1987) and the Galactic center (Gatley et al. 1984). Although less numerous, fluorescent H_2 sources have been found in reflection nebulae (Sellgren 1986; Gatley et al. 1987), the photodissociation region of the Orion bar (Hayashi et al. 1985), the planetary nebula Hubble 12 (Dinerstein et al. 1988) and the extragalactic H II region nebula Hubble 12 (Dinerstein et al. 1988) and the extragalactic H II region NGC 604 in M33 (Israel et al. 1989).

Until recently, the relatively small or undetected 2–1 *S*(1) line in most galaxies was interpreted as strong evidence for thermal

excitation associated with shocks driven by supernova remnants, cloud-cloud collisions or galactic winds. However, recent theoretical development has challenged this interpretation. Sternberg & Dalgarno (1989) have shown that at sufficiently high density ($n_H > 10^4$ cm^{-3}), fluorescently excited H_2 emission will also have the characteristics of a thermal spectrum, due to the collisional de-excitation of the high vibrational levels. The situation is further complicated by the work of Hollenbach & McKee (1989), who showed that fast dissociative *J*-shocks can produce fluorescent emission if H_2 molecules are reformed, downstream of the shock, in excited vibrational levels. Thus, although H_2 line ratios still provide an important diagnostic for constraining the excitation mechanism, independent information and theoretical considerations of the physical conditions prevailing in H_2 emitting galaxies are also essential for identifying the exciting source of the H_2 emission. The study of Puxley, Hawarden, & Mountain (1990) is a good illustration of this point. They showed, with relatively simple models, that photodissociation regions associated with an ensemble of young stars provide a viable model for explaining the "typical" 1–0 *S*(1)/Brγ ratios observed in starburst galaxies. Although this does not prove that fluorescence is the dominant excitation mechanism in galaxies, it suggests that this mechanism must be seriously considered when interpreting extragalactic H_2 spectra.

What is clear from an observational point of view is that there is as yet no unambiguous detection of *low-density* fluorescence in a galaxy, i.e., no galaxy has been found with a large 2–1 *S*(1)/1–0 *S*(1) line ratio. The report of such detection in several bright spirals (Puxley et al. 1988) is certainly tantalizing but their spectra were obtained at relatively low resolution ($R \sim 100$) which makes the assignment of the continuum around the 1–0 *S*(0) and 2–1 *S*(1) very difficult, and this can be misleading for estimating line ratios (Joseph 1989; Moorwood & Oliva 1989). In the following we present evidence that NGC 3256 might be an example of a galaxy in which low-density fluorescence contributes significantly to the bulk of the H_2 emission. This conclusion is based not only from the observed line ratios but also from theoretical considerations of the physical conditions prevailing in the galaxy.

2. THE H_2 SPECTRUM OF NGC 3256

The observations used in this paper have been described in Paper I. *K*-window spectra were obtained on three spatial positions including the nucleus. The 1–0 *S*(1) line of H_2 was detected at every position observed. Because of its better quality, only the spectrum of the nucleus will be used in the forthcoming analysis. We emphasize that all the results described in the next sections apply only for the nucleus.

Figure 1 shows a continuum-subtracted spectrum of NGC 3256 ranging from 2.0 to 2.3 μm (in the rest frame of the galaxy), adapted from the original spectrum presented in Figure 2*a* of Paper I. The continuum was determined by fitting a power law ($F_\lambda \propto \lambda^\beta$) from featureless sections of the spectrum, defined so as to avoid the spectral range of prominent (or potential) emission and absorption lines. The choice of featureless sections of the continuum was guided by the following considerations. Since the nuclear spectrum of NGC 3256 shows a strong CO band (cf. Paper I) typical of late-type stars, the continuum sections were chosen by inspecting the high-resolution spectra from the Kleinmann & Hall's atlas (1986). In late-type stars, the strongest absorption features observed in the *K* band are the CO band longward of 2.3 μm, the Na I

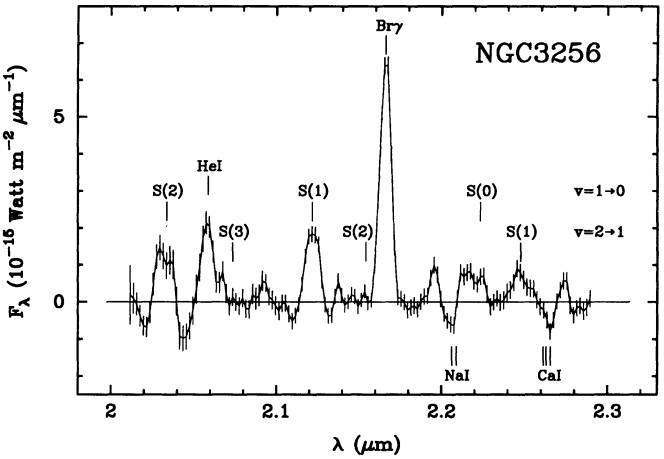

FIG. 1.—*K*-window spectrum of the nucleus of NGC 3256 obtained with an aperture of 3″.5 × 3″.5. The underlying continuum has been subtracted as described in the text. The spectrum is shown in the restframe of the galaxy. Each spectral point is plotted with an error bar of $\pm 1\ \sigma$. Adopted from Paper I.

doublet ($\sim$2.206 μm) and the Ca I triplet ($\sim$2.263 μm). As noted in Paper I, the apparently strong absorption features at $\sim$2.02 and $\sim$2.045 μm are most likely the result of an imperfect correction of a strong CO_2 atmospheric feature, and hence, those spectral regions were excluded for defining the continuum. The emission lines avoided are He I 2.06, Brγ (2.166 μm), and several transitions of H_2 including the 1–0 *S*(0) (2.223 μm, 1–0 *S*(1) (2.122 μm), 1–0 *S*(2) (2.034 μm), 2–1 *S*(1) (2.248 μm), 2–1 *S*(2) (2.154 μm), and the 2–1 *S*(3) (2.074 μm). The final spectral intervals used to define the continuum are centered at 2.075, 2.143, 2.235, and 2.285 μm.

After Brγ, the dominant emission feature in the spectrum is the 1–0 *S*(1) transition of H_2 but other H_2 transitions are also detected, including the 1–0 *S*(2), 1–0 *S*(0), 2–1 *S*(1), and the first three transitions of the 1–0 *Q*-branch (not shown here, cf. Paper I). Adopting a distance of 37 Mpc for NGC 3256, the 1–0 *S*(1) flux of 1.8×10^{-17} W m^{-2} observed in the central

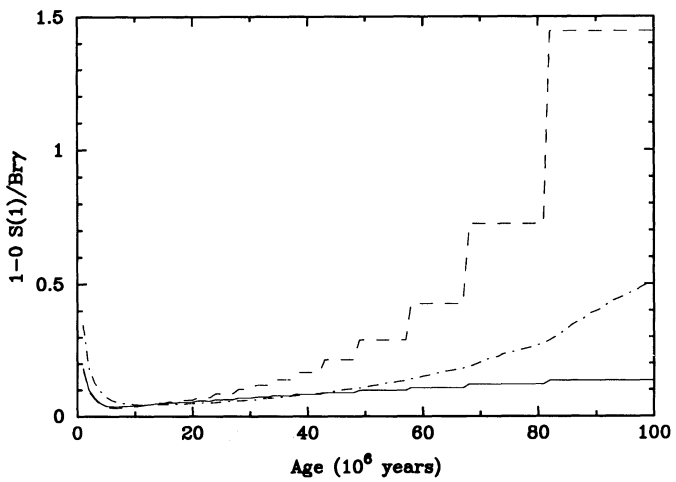

FIG. 2.—Evolution of the 1–0 *S*(1)/Brγ line ratio with time calculated as described in the text. The three curves correspond to different star formation rates: constant (*solid line*), exponential (*dashed line*), and "delayed" (*dash-dotted line*). The last two SFR were calculated with a time scale $\tau = 20 \times 10^6$ yr.

3″.5 × 3″.5 of the nucleus (cf. Table 1 of DJW) corresponds to a luminosity $L_{S(1)} = 7.7 \times 10^5\ L_\odot$ which increases to $2 \times 10^6\ L_\odot$ when the 1–0 $S(1)$ flux detected in two other apertures outside the nucleus (cf. Paper I). This latter estimate is obviously a lower limit of the total 1–0 $S(1)$ luminosity since the mapping of the galaxy was incomplete. For comparison, the integrated H_2 luminosity of NGC 3256 is, at least an order of magnitude brighter than that observed in the nearby starburst M82 [$L_{S(1)} = 2 \times 10^5\ L_\odot$; Lester et al. 1990], comparable to the ultraluminous *IRAS* galaxy Arp 220 [$L_{S(1)} = 4 \times 10^6\ L_\odot$; Joseph, Wright, & Wade 1984] but far behind NGC 6240 [$L_{S(1)} = 4.5 \times 10^7\ L_\odot$; Joseph, Wright, & Wade 1984]. It is worthwhile to note that, despite the wide range of H_2 luminosity observed in NGC 3256, Arp 220, and M82, they all have a very similar 1–0 $S(1)$ surface brightness near $2\ L_\odot\ pc^{-2}$. NGC 6240 is in an class of its own with an H_2 surface brightness greater than $10\ L_\odot/pc^2$.

3. EXCITATION MECHANISM OF THE H_2 EMISSION

3.1. *Constraints from Line Ratios*

The H_2 line ratios observed on the nucleus of NGC 3256 are presented in Table 1 and compared with predictions from typical shock and low-density fluorescent models taken from Black & Van Dishoeck (1987). This table shows that it is difficult to fit all the observed line ratios with either a shock or UV fluorescence model. Indeed, the strength of the 2–1 $S(1)$ is too strong for shock excitation and more consistent with UV excitation. On the other hand, the UV fluorescence model predicts a 2–1 $S(3)$ which is twice as strong as our 3 σ upper limit. We note that an acceptable fit would be obtained with the shock model if the 2–1 $S(1)$ would be excluded from the analysis. A better fit is obtained if we empirically assume a "mixed" model in which half of the H_2 emission in the K-window is radiatively excited and the rest excited by shock. As shown in Table 1, a mixed model is consistent with the both undetected 2–1 $S(3)$ and 1–0 $S(2)$ and the equally strong 2–1 $S(1)$ and 1–0 $S(0)$.

Since the only evidence for low-density fluorescence relies on the correct identification and detection of the 2–1 $S(1)$, some remarks are in order about this line. We can rule out the possibility that we have overestimated the strength of the 2–1 $S(1)$ by misplacing the local continuum. Although, there are still uncertainties in the assignment of the continuum, the resolution of the spectrum shown in Figure 1 is high enough to detect the Na I and Ca I absorption next to the 1–0 $S(0)$ and 2–1 $S(1)$ lines. DJW showed in Paper I that the strength of the CO band in the nucleus implies that 2.2 μm luminosity is dominated by late-type stars, an interpretation which is confirmed by the fact that the Na I and Ca I lines have equivalent widths very similar to that observed in late-type giants. This confirms that our assignment of the continuum near the 2–1 $S(1)$ is very reasonable. It was mentioned in Paper I that some of the wiggles and bumps in the spectrum could be spuriously produced by a bad cancellation of atmospheric OH lines. We can certainly rule out this possibility for the 2–1 $S(1)$ because there is a cutoff at 2.25 μm beyond which the OH lines disappear and the 2–1 $S(1)$ was observed at 2.269 μm (before shifting the spectrum in the restframe). The same argument applies for the Ca I triplet absorption feature.

Equally important is the assignment of the continuum near the 1–0 $S(1)$. We cannot rule out the possibility that we have overestimated the continuum near this line 1–0 $S(1)$ given the small dips observed on both sides (see Fig. 1). However, we suggested in Paper I that the depression of the continuum on the blue side of the 1–0 $S(1)$ could be identified with Al/Mg. This motivated our choice of excluding this dip for defining the continuum. In any case, even we make the extreme assumption that the local continuum around the 1–0 $S(1)$ passes through the bottom of the dips, the resulting 2–1 $S(1)$/1–0 $S(1)$ ratio would decrease from 0.39 to 0.32, which is still much too high for shock excitation.

The evidence for low-density fluorescence from the strong 2–1 $S(1)$ is obviously marginal and confirmation of this result from a higher resolution spectrum is certainly needed.

An important test of low-density fluorescence is to look for high vibrational H_2 lines in the J and H windows. These lines are predicted to have intensities similar to the K-window transitions (Black & Van Dishoeck 1987; Sternberg & Dalgarno 1989). Using the theoretical line ratios of Black & van Dishoeck (1987), we have calculated synthetic J and H H_2 spectra at the same resolution as the corresponding spectra obtained on NGC 3256 (cf. Paper I). The line intensities were scaled with the observed strength of the 1–0 $S(1)$ and corrected for reddening assuming an absolute extinction at 2.2 μm of 0.55 mag (as derived in Paper I) and the extinction law of Draine (1989). The resulting synthetic H_2 spectrum was then compared with the observed J and H band spectra of NGC 3256 (cf. Paper I). We found that the synthetic H_2 spectrum is virtually buried in the noise, and therefore, no constraints can be put on the excitation mechanism from the J and H band spectra. Thus, although J and H H_2 lines provide in principle the best diagnostic for determining the excitation mechanism, in practice these transitions can be very difficult to detect because of the extinction.

Since the H_2 K spectrum of NGC 3256 is best explained by a mixture of fluorescent and shock excitation, we investigate in the following sections how we can constrain, from a theoretical point of view, the relative amount of H_2 emission excited by shock and UV fluorescence.

TABLE 1

H_2 LINE RATIOS IN NGC 3256

LINE	λ[a] (μm)	I/I_0[b]	MODEL		
			Shock[c]	UV[c]	Mixed[d]
1–0 $S(2)$.....	2.0338	0.45 ± 0.13	0.37	0.50	0.44
2–1 $S(3)$.....	2.0735	<0.17	0.08	0.35	0.22
1–0 $S(1)$[e].....	2.1218	1.00	1.00	1.00	1.00
2–1 $S(2)$.....	2.1542	<0.17	0.03	0.28	0.16
1–0 $S(0)$.....	2.2233	0.26 ± 0.05	0.21	0.46	0.34
2–1 $S(1)$.....	2.2477	0.39 ± 0.06	0.08	0.56	0.32

[a] Wavelength in vacuum.

[b] Corrected for extinction ($A_K = 0.55$ mag; cf. Paper I). 3 σ upper limits are given for undetected lines.

[c] Shock and UV line ratios from Black & Van Dishoeck 1987 model S2 and model 14.

[d] Expected line ratios assuming equal contribution of 1–0 $S(1)$ flux from shock and UV excited H_2 gas.

[e] The observed line flux is 1.8×10^{-17} W m^{-2} or 3.1×10^{-17} W m^{-2}, corrected for extinction.

3.2. H_2 *Emission Contribution from a Shock Component*

Since the most common sources of shock-excited H_2 emission in our Galaxy are associated with young stellar objects and supernova remnants, it is natural to suppose that these

sources should have a certain contribution to the integrated H_2 luminosity of a starburst galaxy like NGC 3256. Whether this contribution is significant or not is what we will try to estimate here.

In order to estimate the H_2 contribution of these sources, one needs to know their intrinsic H_2 luminosities and their lifetimes. The best-studied young stellar objects are the Orion nebula, DR 21, Cepheus A, and NGC 2071 which have been measured to have a 1–0 $S(1)$ luminosity, corrected for extinction, of 6 $L_\odot$ (Burton & Puxley 1989), 180 $L_\odot$ (Garden et al. 1986), 1.2 $L_\odot$ (Doyon & Nadeau 1988), and 1.1 $L_\odot$ (Lane & Bally 1986), respectively. The figure for DR 21 is very uncertain because its distance is known only within 30%. Taking the weighted average of these luminosities, weighting DR 21 with half the weight assigned the other sources, yields an average 1–0 $S(1)$ luminosity $L^{\rm YSO}_{S(1)} \sim 30\ L_\odot$. The lifetimes of these sources can be estimated from the ratio of the spatial extent of the H_2 emission to the shock velocity. More sophisticated techniques based on this principle yield a lifetime of $\sim 10^4$ yr (Fischer et al. 1985; Oliva & Moorwood 1986).

There are at present four supernova remnants where the H_2 emission has been detected, namely IC 443 (Graham, Wright, & Longmore 1987; Burton et al. 1988), RCW 103 (Oliva, Moorwood, & Danziger 1989), the Crab Nebula (Graham, Wright, & Longmore 1990) and the Cygnus Loop (Graham et al. 1991). The integrated 1–0 $S(1)$ luminosities of these sources are 70 $L_\odot$ for IC 443, 60–90 $L_\odot$ for RCW 103 and less than 1 $L_\odot$ for the Crab Nebula and the Cygnus Loop; all values have been corrected for extinction except for RCW 103. Most of these luminosities are somewhat uncertain since a relatively small fraction of the total remnants were mapped in general. Remnants in the LMC are not plagued by this problem. Oliva, Moorwood, & Danziger (1989) detected the [Fe II] emission in three LMC remnants and provided upper limits for the 1–0 $S(1)$ line corresponding to luminosities between 3 and 70 $L_\odot$. This is consistent with the luminosities of galactic remnants. Both IC 443 and RCW 103 are remnants expanding in a molecular cloud, whereas the Cygnus Loop has not yet reached this stage; the remnant is still expanding in the normal diffuse interstellar medium (ISM). Since high concentration of molecular gas is often observed in starburst galaxies, IC 443 and RCW 103 are probably more representative of the typical SNR associated with these galaxies. We thus adopt a value of 70 $L_\odot$ as the typical 1–0 $S(1)$ luminosity of SNRs in starbursts. As for the lifetime of the remnants, we adopt the age of IC 443 estimated to be 1.3×10^4 yr (Parkes, Culhane, & Ives 1977).

These numbers can now be used along with the evolutionary starburst model described in Paper I to estimate the integrated H_2 luminosity associated with YSOs and SNRs. The model follows the evolution of stars in the H-R diagram according to known evolutionary tracks, for a given IMF and a birth rate function. We assume that all stars more massive than 6 $M_\odot$ experience a YSO phase at their formation, emitting a constant 1–0 $S(1)$ luminosity of 30 $L_\odot$ for a period of 10^4 yr. It also assumed that these stars will become Type II supernovae at the end of their life, their remnants emitting a 1–0 $S(1)$ luminosity of 70 $L_\odot$ for a period of 1.3×10^4 yr. Since the model also provides the Brγ luminosity from the ionization rate, we can then predict the 1–0 $S(1)$/Brγ ratio associated with YSOs and SNRs as a function of time.

Although the intrinsic luminosities and time scales of these sources are uncertain, there are reasons to believe that the 1–0 $S(1)$/Brγ ratio predicted by our simple calculation will probably be overestimated. First, in deriving the 1–0 $S(1)$/Brγ we implicity assumed that the extinction towards the molecular and ionized gas is the same. This is probably conservative since the H_2 emission associated with YSOs and SNRs arises from regions deep in molecular clouds with typical visual extinction of 20 mag whereas the young OB stars contributing to the ionization are mostly located, on average, in the diffuse interstellar medium (ISM). Indeed, comparison of the relative number of compact H II regions and O stars in our Galaxy shows that the latter spend only 15% of their lifetime embedded in their parent molecular cloud (Wood & Churchwell 1989). Thus, it is likely that the Brγ emission suffers considerably less extinction than the 1–0 $S(1)$ line. Second, it is probably too optimistic to assume that the H_2 luminosity is constant over the lifetime of YSOs and SNRs. The H_2 luminosity of an SNR should drastically increase when the remnant hits a molecular cloud (like IC 443) after a previous stage of expansion in the diffuse ISM (like the Cygnus loop).

The evolution of the 1–0 $S(1)$/Brγ ratio as a function of time is shown in Figure 2. The models were calculated with a Scalo (1986) IMF and a lower and upper mass limits of 0.1 and 30 $M_\odot$, respectively. Note that these calculations include H_2 emission contributions from YSOs and SNRs only. The effect of the star formation rate (SFR) on the line ratio was investigated with three birthrate functions: constant, exponential (SFR $\propto \exp^{-t/\tau}$) and "delayed" (SFR $\propto t \exp^{-t/\tau}$). For the latter two birthrate functions, an arbitrary time scale τ of 20 million years was assumed. For the first 10 million years, the H_2 luminosity is dominated by YSOs and apart from the very early stage of the burst (<5 million years), the 1–0 $S(1)$/Brγ is ~ 0.05. The ratio increases around 30 million years because of the increasing contribution of H_2 emission from SNRs and the rapidly decreasing Brγ flux. These calculations show that, for a single-event starburst, large 1–0 $S(1)$/Brγ ratios in the range of 0.05–1, as typically observed in star-forming galaxies (e.g., Moorwood & Oliva 1988; Puxley et al. 1988) are possible *only if the age of the burst is greater than 30 million years and the SFR is exponentially decreasing.* As shown in Paper I, the Brγ equivalent width can be used as an age indicator. For an upper mass limit of 30 $M_\odot$, a burst age greater than 30 million years corresponds to a Brγ equivalent width smaller than ~ 10 Å (cf. Fig. 4 of Paper I).

For an age between 12 and 27 million years, as derived in Paper I for NGC 3256, the 1–0 $S(1)$/Brγ is predicted to be 0.05–0.1, much lower than the ratio of 0.34 ± 0.02 observed on the nucleus. This implies that only 20%–30% of the H_2 emission at this position is contributed by YSOs and SNRs. On the basis of these calculations we conclude that, although YSOs and SNRs are unlikely to be the main sources of H_2 emission in NGC 3256, their contribution to the H_2 luminosity observed in the K window is not negligible.

Another potential source of collisionally excited H_2 emission is that associated with large-scale shocks driven by the merger of the two parent galaxies in NGC 3256. This mechanism is probably responsible for the strong H_2 emission observed in the merger NGC 6240. Line imaging of this galaxy (Herbst et al. 1990) has revealed that the peak of the H_2 emission is displaced from the two infrared nuclei, a feature that was interpreted as evidence that large-scale shocks are responsible for the excitation of the H_2 gas. Interestingly, we find that the H_2 emission in NGC 3256 is equally strong on the nucleus and 5″ south (Paper I). Although a detailed mapping/imaging of this galaxy is needed to accurately determine the relative extent of

the H_2 emission and the continuum, our observations are very suggestive that, like NGC 6240, the H_2 peak is not exactly coincident with the infrared nucleus, and hence, a certain fraction of the K-window H_2 emission is associated with large-scale shocks. More H_2 observations at higher spatial resolution are needed to assess further this question.

3.3. H_2 *Emission Contribution from UV Fluorescence*

Conspicuous production of UV photons is a natural consequence of vigorous star formation activity. If there is enough molecular material in the vicinity of young OB stars then the UV radiation field will interact with the molecular gas and produce fluorescent H_2 emission. Fischer et al. (1987) and Puxley et al. (1988) have used a simple criterion to show that fluorescence is indeed a viable mechanism for explaining the H_2 emission in some AGNs and starburst galaxies. More recently, Puxley et al. (1990) have shown how typical 1–0 $S(1)$/Brγ ratios observed in star-forming galaxies can be explained by fluorescence. In particular, they showed that this ratio depends critically on the geometry of the emitting regions. In this section, we investigate whether UV fluorescence provides a viable mechanism for exciting a significant fraction of the H_2 gas in NGC 3256.

We suppose that the emitting region of the starburst is made of $N_{\rm cl}$ spherical molecular clouds of mass $M_{\rm H_2}^{\rm cl}$ and density n. These clouds are bathed in a diffuse UV radiation field produced by recently formed OB stars which are assumed to be located in the diffuse interstellar medium, outside their parent molecular clouds. This geometry corresponds to "Model C" of Puxley et al. (1990) and is justified by the fact that the nucleus of NGC 3256 is relatively evolved, even if the starburst is not older than 15 million years. The fact that galactic O stars spend only 15% of their lifetimes embedded in their parent molecular clouds (Wood & Churchwell 1989) suggests this geometry is probably a good representation of the interstellar medium of the nuclear region of NGC 3256.

The UV radiation field impinging on molecular clouds produces fluorescent H_2 emission. For an observer at a distance D, the integrated H_2 flux emitted in the 1–0 $S(1)$ line from all the clouds in the beam is given by

$$F_{S(1)} = 4\pi R_{\rm cl}^2 \left(\frac{M_{\rm H_2}^{\rm tot}}{M_{\rm H_2}^{\rm cl}}\right) I_{S(1)} D^{-2} , \quad (1)$$

where $R_{\rm cl}$ is the radius of the clouds, $M_{\rm H_2}^{\rm tot}$ the total H_2 mass in the beam and $I_{S(1)}$, the intensity of the fluorescent 1–0 $S(1)$ line in units of W m^{-2} sr^{-1}. The following analytical expression can be used for this intensity (Sternberg 1989):

$$I_{S(1)} = 5.1 \times 10^{-13} \left(\frac{\sigma_0}{\sigma}\right)\left(\frac{R}{R_0}\right) n \times \ln\left[90\left(\frac{\sigma_0}{\sigma}\right)^{1/2}\left(\frac{R}{R_0}\right)\left(\frac{\chi}{n}\right) + 1\right], \quad (2)$$

where χ is the photon flux between 912 and 1108 Å, relative to the mean background of 2.7×10^{11} photons s^{-1} m^{-2} measured in the solar neighborhood (Draine 1978, as quoted in Black & Van Dishoeck 1987). The parameter R is the molecular formation rate coefficient and σ the effective dust continuum cross section at 1000 Å, with $R_0 = 3 \times 10^{17}$ cm^3 s^{-1} and $\sigma_0 = 1.9 \times 10^{-21}$ cm^2. After substitution of equation (1) in equation (2), assuming $R_{\rm cl} = 3M_{\rm H_2}^{\rm cl}/4\pi n m_{\rm H})^{1/3}$ ($m_{\rm H}$ is the mass of a hydrogen atom), $R = R_0$ and $\sigma = \sigma_0$, we have

$$F_{S(1)} = 1.35 \times 10^{-15} \left(\frac{M_{\rm H_2}^{\rm tot}}{10^8\, M_\odot}\right)\left(\frac{M_{\rm H_2}^{\rm cl}}{10^5\, M_\odot}\right)^{-1/3}\left(\frac{n}{10^4\ {\rm cm}^{-3}}\right)^{1/3} \times \left(\frac{D}{\rm Mpc}\right)^{-2} \ln\left[90\left(\frac{\chi}{n_{\rm H}}\right) + 1\right] {\rm W\ m}^{-2} . \quad (3)$$

The three unknown quantities in this equation are the mass of individual clouds $M_{\rm H_2}^{\rm cl}$, the density n and the intensity of the UV field χ. For the total H_2 mass in the beam, $M_{\rm H_2}^{\rm tot}$, we adopt the estimate of $1.8 \times 10^8\ M_\odot$ derived from the CO map of Sargent, Sanders, & Phillips (1989) (see also § 4.3 of Paper I). Given the observed H_2 flux (3.1×10^{-17} W m^{-2}, corrected for extinction) and a distance of 37 Mpc, the values of n and χ are constrained by the implicit equation

$$\left(\frac{M_{\rm H_2}^{\rm cl}}{10^5\, M_\odot}\right)^{-1/3}\left(\frac{n}{10^4\ {\rm cm}^{-3}}\right)^{1/3} \ln\left[90\left(\frac{\chi}{n}\right) + 1\right] = 17.45f \quad (4)$$

where f is the fraction of the total H_2 emission excited by fluorescence. This constraint is graphically displaced in Figure 3 for $f = 1$ (solid lines) and $f = 0.5$ (dashed lines), calculated with molecular cloud masses of 10^3, 10^4 and $10^5\ M_\odot$.

Although it is difficult to constrain the density, one can still put an upper limit on this parameter from the 2–1 $S(1)$/1–0 $S(1)$ line ratio. If we assume that all the H_2 emission is fluorescently excited, then this ratio will vary from 0.56 in the low-density regime ($\sim 10^4$ cm^{-3}) to 0.1 when the density reaches $\sim 10^5$ cm^{-3} (Sternberg & Dalgarno 1989). The ratio of 0.4 observed on the molecules of NGC 3256 implies an excitation temperature of $\sim$4500 K, and from Figure 12 of Sternberg & Dalgarno (1989), this corresponds to a density of (2–3) $\times 10^4$ cm^{-3} (log $n = 4.4$).

It follows from Figure 3 that the minimum intensity of the UV field that could produce half of the total 1–0 $S(1)$ emission is log $\chi = 2.7$ assuming that the average molecular cloud in the center of NGC 3256 has a mass of $10^3\ M_\odot$. Overall, cloud masses between 10^3 and $10^4\ M_\odot$ and log $\chi = 3$–5 could easily explain at least half if not all of the observed H_2 emission.

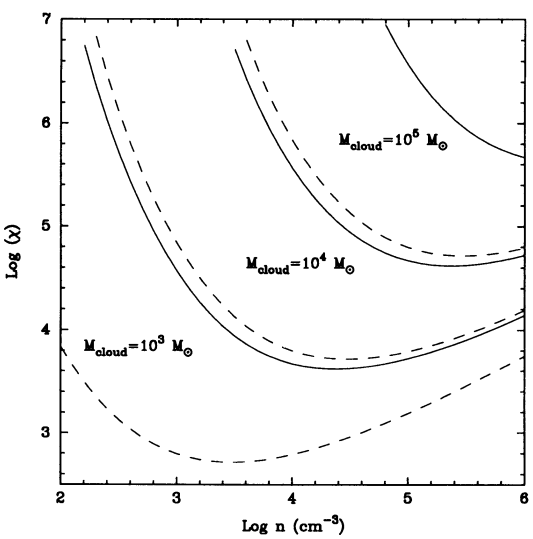

FIG. 3.—Constraints on the intensity of the UV field χ and the density n for producing all (*solid line*) or half (*dashed line*) of the observed 1–0 $S(1)$ H_2 flux by UV fluorescence, each case calculated with three different molecular cloud masses.

We now try to estimate the UV intensity in the center of NGC 3256. The UV intensity χ at a distance d from star with effective temperature $T_{\rm eff}$ is given by

$$\chi = 310\left(\frac{N_{\rm NUV}(T_{\rm eff})}{10^{48}\ {\rm s}^{-1}}\right)\left(\frac{d}{\rm pc}\right)^{-2}, \quad (5)$$

where $N_{\rm NUV}(T_{\rm eff})$ is the production rate of non-ionizing photons between 912 and 1108 Å. Puxley et al. (1990) have calculated this parameter for stars of different effective temperatures by integrating under Kurucz (1979) atmosphere models. For an O8V star ($T_{\rm eff} \sim 35{,}000$ K), which is the average spectral type of the ionizing stars in NGC 3256 (see § 4.1 of Paper I), $N_{\rm NUV} = 4 \times 10^{48}\ {\rm s}^{-1}$.

One can obtain a lower limit on χ by evaluating equation (5) at one-half the mean separation of ionizing stars. Assuming that the stars are uniformly distributed, this separation is

$$\frac{d_*}{2} = 0.62\rho_*^{-1/3}\ {\rm pc}, \quad (6)$$

where ρ_* is the number of ionizing stars per cubic parsec. The number of O8V stars in NGC 3256 is estimated (cf. Paper I) to be 7×10^5, yielding $\rho_* = 0.01$ or $0.02\ {\rm pc}^{-3}$ depending on whether the total volume is a sphere of 300 pc in radius or a disk of the same diameter with a thickness of 100 pc. This yields a one-half mean separation of 2–3 pc, corresponding to $\log \chi = 2.1$–2.5.

A more realistic estimate of χ is obtained by integrating the UV intensity of all the stars in the nucleus. One must take into account the effect of dust absorption in the interstellar medium. At a distance d from a star, the UV intensity is simply given by $\chi(d) = \chi_0 \exp(-n_{\rm H}^{\rm ism}\sigma_0 d)$, where χ_0 is the UV intensity if there were no dust and $n_{\rm H}^{\rm ism}$ is the neutral density of the diffuse ISM. For instance, for a typical ISM density of $1\ {\rm cm}^{-3}$, and optical depth of one corresponds to a distance of 170 pc. Thus, there is clearly more than one star contributing to the UV intensity at a given point in the nucleus. Integrating over large distances and taking into account the effect of dust absorption, we then have

$$\chi = 13{,}000\left(\frac{\bar{N}_{\rm NUV}}{10^{48}\ {\rm s}^{-1}}\right)\left(\frac{\rho_*}{10^{-2}\ {\rm pc}^3}\right)\left(\frac{n_{\rm H}^{\rm ism}}{1\ {\rm cm}^{-3}}\right)^{-1} \times \left(\frac{\sigma_0}{10^{-21}\ {\rm cm}^2}\right)^{-1} \quad (7)$$

where $\bar{N}_{\rm NUV}$ is the average number of non-ionizing photons per star. This expression is valid as long as the obscuration is dominated by dust in the interstellar medium and not by dust in molecular clouds. Assuming that the H_2 clouds have an average mass of $10^4\ M_\odot$, then the total H_2 mass in the nucleus implies a one-half mean cloud separation of 7–10 pc, 3 times the separation of the stars. Assuming a cloud density of $10^4\ {\rm cm}^{-3}$, these clouds would have a radius of 2 pc. In such conditions, only 2% of the volume would be filled by molecular clouds. We can quantify the obscuration effect due to molecular clouds by estimating the distance beyond which the total solid angle of the clouds is greater than 2π sr, i.e., when they cover half the sky from any location in the nucleus. This distance is given by $r_0 = 1/2\pi\rho_{N_{\rm cl}}R_{\rm cl}^2$, where $\rho_{N_{\rm cl}}$ is the number of molecular clouds per cubic parsec. Using the numbers above, this distance is $\sim$100–200 pc. This is of the same order as the distance at which the dust optical depth is one, and shows that it is reasonable to assume that the obscuration is dominated by dust.

Equation (7) shows that UV intensities of the order of 10^4 are certainly possible in the nucleus of NGC 3256, and as shown in Figure 3, such intensity is high enough to produce more than half of the observed H_2 emission. In fact, this estimate could well be underestimated since we have assumed a uniform stellar distribution. In reality, young stars are usually found closer to their parent molecular clouds, resulting in strong radiation field at their surfaces. The best example of such situation is the Orion nebula where the UV intensity near the photodissociation region (the Orion bar) is estimated to be 10^5 times the Galactic background.

This simple analysis shows that UV fluorescence is a viable mechanism for explaining at least half of the 1–0 $S(1)$ emission observed in the nucleus of NGC 3256, provided that the neutral density in molecular clouds is high enough ($\sim 10^4\ {\rm cm}^{-3}$) and that their masses are $\lesssim 10^4\ M_\odot$, a requirement which is very reasonable. This conclusion is consistent, at least qualitatively, with the observed line ratios which suggest that half of the H_2 emission in the K-window is fluorescently excited (cf. § 3.1).

4. DISCUSSION AND CONCLUDING REMARKS

The main conclusion that can be drawn from our analysis is that it is difficult to explain the H_2 spectrum of NGC 3256 with a single excitation mechanism, either shock or fluorescence. The observations are better reproduced when both excitation mechanisms are involved. The simple calculations presented before suggest that a natural consequence of starburst activity is to produce *both* shock- and fluoresently excited H_2 emission in appreciable quantities, sufficient to explain the observed H_2 spectrum. The relative fraction of thermal and nonthermal H_2 emission depends on several physical parameters. The geometry of the photodissociation regions, the concentration of the molecular gas and the intensity of the star formation rate partly determined the amount H_2 emission excited by UV fluorescence. The age of the burst and the star formation rate history are important parameters determining the contribution of shock-excited H_2 emission associated with YSOs and SNRs.

It is important to stress that the relative fraction of UV and shock-excited H_2 emission derived from a K-window H_2 spectrum is totally different from that inferred when the *total* emission (emitted at all wavelengths) is considered. Since only 1% of the total H_2 emission excited by UV fluorescence is emitted in the 1–0 $S(1)$ line as opposed to 10% for shock excitation (cf. Black & van Dishoeck 1987), UV fluorescence must contribute a relatively large fraction of the total H_2 emission in order to imprint its nonthermal spectral signature in the K window. Taking NGC 3256 as an example, the fact that at least half of the H_2 emission emitted in the K window is fluorescently excited implies that UV fluorescence is responsible for more than 90% of the total H_2 emission observed in this galaxy. Thus, when the total H_2 emission is considered, UV fluorescence is by far the dominant excitation mechanism of the H_2 gas in NGC 3256.

This work shows how the K-window H_2 spectrum can be misleading for constraining the excitation mechanism of the H_2 gas in a situation where the H_2 emission is made of two components: thermal and nonthermal. In such case, the K-window H_2 transitions are mostly sensitive to the thermal component of the H_2 spectrum. To illustrate this point further, let us consider a hypothetical galaxy in which the total H_2

emission would be equally contributed by shocks and UV fluorescence. The H_2 spectrum of this galaxy would show a 2–1 $S(1)$/1–0 $S(1)$ ratio of 0.14, much closer to the theoretical ratio of 0.1 expected for shock excitation (0.56 for UV fluorescence). Unless very accurate, extinction corrected line ratios would be available for this galaxy, it would be extremely difficult to determine the fraction of H_2 emission excited by UV fluorescence, and one could easily conclude that shocks is the dominant excitation mechanism even though UV fluorescence contributes half of the total H_2 emission. In this context, one must be very careful to draw conclusions about the dominant excitation mechanism in starburst galaxies in general, especially when those are drawn from moderate signal-to-noise observations of a few H_2 transitions in the K window, which is the case for most H_2 spectra observed thus far in starbursts. The fact that most starburst galaxies apparently show thermal H_2 spectra in the K-window does not necessarily imply that shocks represent the dominant excitation mechanism of the H_2 emission, it only means that a significant fraction of the total H_2 emission is shock-excited. A nonnegligible fluorescence component could easily be hidden in the spectrum, especially if the extinction is important. This could be the case for instance of Arp 220 and M82, two starburst galaxies for which the observed H_2 emission is generally thought to be shock-excited. The fact that both galaxies have a H_2 surface brightness similar to NGC 3256 (cf. § 2) might be a hint—although speculative—that a nonnegligible fraction of the total H_2 emission is fluorescently excited in Arp 220 and M82.

It is a pleasure to thank D. Allen, P. Meikle and J. Spyromilio for their help in taking the observations on the AAT. We would like to thank J. Black, who made us aware of the Aalto et al. paper on the properties of the molecular gas in NGC 3256. We are also grateful to the anonymous referee for very useful suggestions. R. D. is financially supported by a postdoctoral NSERC fellowship.

REFERENCES

Black, J. H., & Dalgarno, A. 1976, ApJ, 203, 132
Black, J. H., & van Dishoeck, E. F. 1987, ApJ, 322, 412
Brand, P. W. J. L., Moorhouse, A., Burton, M. G., Geballe, T. R., Bird, M., & Wade, R. 1988, ApJ, 334, L103
Burton, M. G., Geballe, T. R., Brand, P. W. J. L., & Webster, A. S. 1988, MNRAS, 231, 617
Burton, M. G., & Puxley, P. J. 1989, preprint
DePoy, D. L., Becklin, E. E., & Wynn-Williams 1986, ApJ, 307, 116
Dinerstein, H. L., Lester, D. F., Carr, J. S., & Harvey, P. M. 1988, ApJ, 327, L27
Doyon, R., Joseph, R. D., & Wright, G. S. 1994, ApJ, 421, 101
Doyon, R., & Nadeau, D. 1988, ApJ, 334, 883
Draine, B. T. 1978, ApJS, 36, 595
———. 1989, in Proc. 22d ESLAB Symp. Infrared Spectroscopy in Astronomy, ed. B. H. Kaldeich (Paris: ESA Pub. Div.), 93
Elias, J. H. 1980, ApJ, 241, 728
Fischer, J., Geballe, T. R., Smith, H. A., Simon, M., & Storey, J. W. V. 1987, ApJ, 320, 667
Fischer, J., Sanders, D. B., Simon, M., & Solomon, P. M. 1985, ApJ, 293, 504
Garden, R., Geballe, T. R., Gatley, I., & Nadeau, D. 1986, MNRAS, 220, 203
Gatley, I., Hasegawa, T., Suzuki, H., Garden, R., Brand, P., Lightfoot, J., Glenncross, W., Okuda, H., & Nagata, T. 1987, ApJ, 318, L73
Gatley, I., Jones, T. J., Hyland, A. R., Beattie, D. H., & Lee, T. J. 1984, MNRAS, 210, 565
Gautier III, T. N., Fink, U., Treffers, R., & Larson, H. P. 1976, ApJ, 207, L129
Graham, J. R., Wright, G. S., Hester, J. J., & Longmore, A. J. 1991, AJ, 101, 175
Graham, J. R., Wright, G. S., & Longmore, A. J. 1987, ApJ, 313, 847
———. 1990, ApJ, 352, 172
Hall, D. N. B., Kleinmann, S. G., Scoville, N. Z., & Ridgway, S. T. 1981, ApJ, 248, 898
Hayashi, M., Hasegawa, T. Geballe, T. R., Garden, R., & Kaifu, N. 1985, MNRAS, 215, 31P
Herbst, T. M., Graham, J. R., Beckwith, S., Tsutsui, K., Soifer, B. T., & Matthews, K. 1990, AJ, 99, 1773
Hollenbach, D., & Shull, J. M. 1977, ApJ, 216, 419
Hollenbach, D., & McKee, C. F. 1989, ApJ, 342, 306
Israel, F. P., Hawarden, T. G., Wade, R., Geballe, T. R., & Van Dishoeck, E. F. 1989, MNRAS, 236, 89
Joseph, R. D. 1989, in Proc. 22d ESLAB Symp. Infrared Spectroscopy in Astronomy, ed. B. H. Kaldeich (Paris: ESA Pub. Div.), 439
Joseph, R. D., Wright, G. D., & Wade, R. 1984, Nature, 311, 132
Kawara, K., Nishida, M., & Gregory, B. 1987, ApJ, 321, L35
Kleinmann, S. G., & Hall, D. B. 1986, ApJS, 62, 501
Kurucz, R. L. 1979, ApJS, 40, 1
Lane, A. P., & Bally, J. 1986, ApJ, 310, 820
Lester, D. F., Carr, J. S., Joy, M., & Gaffney, N. 1990, ApJ, 352, 544
Lester, D. F., Harvey, P. M., & Carr, J. S. 1988, ApJ, 329, 641
Moorwood, A. F. M., & Oliva, E. 1988, A&A, 203, 278
———. 1989, in Proc. 22d ESLAB Symp., Infrared Spectroscopy in Astronomy, ed. B. H. Kaldeich (Paris: ESA Pub. Dev.), 507
Oliva, E., & Moorwood, A. F. M. 1986, A&A, 164, 104
Oliva, E., Moorwood, A. F. M., & Danziger, I. J. 1989, A&A, 214, 307
Parkes, C. G. E., Culhane, J. L., & Ives, J. C. 1977, MNRAS, 179, 55
Prestwich, A. H. 1989, Ph.D. thesis, Imperial College, University of London
Puxley, P. J., Hawarden, T. G., & Mountain, M. C. 1988, MNRAS, 234, 29P
———. 1990, ApJ, 364, 77
Rieke, G. H., Cutri, R. M., Black, J. H., Kailey, W. F., McAlary, C. W., Lebofsky, M. J., & Elson, R. 1985, ApJ, 290, 116
Sargent, A. I., Sanders, D. B., & Phillips, T. G. 1989, ApJ, 346, L9
Scalo, J. M. 1986, Fund. Cosmic Phys., 11, 1
Sellgren, K. 1986, ApJ, 305, 399
Sternberg, A. 1989, in 22nd ESLAB Symp., Infrared Spectroscopy in Astronomy, ed. B. H. Kaldeich (Paris: ESA Pub. Div.), 269
Sternberg, A., & Dalgarno, A. 1989, ApJ, 338, 197
Thompson, R. I., Lebofsky, M. J., & Rieke, G. H. 1978, ApJ, 222, L49
Treffers, R. R., Fink, U., Larson, H. P., & Gautier III, T. N. 1976, ApJ, 209, 793
Wood, D. O. S., & Churchwell, E. 1989, ApJ, 340, 265

Note added in proof.—Soon after the completion of this work (end of 1990), new CO observations of NGC 3256 were published by Aalto et al. (A&A, 247, 291 [1991]) who also describe a model of the molecular clouds. They show that the clouds must be relatively small ($r \leq 1$ pc) with masses between 1300 and 1900 $M_\odot$ and densities of (5–7) $\times$ 10^3 cm^{-3}. As shown in Figure 3 of this paper, such a combination of density and mass of the molecular clouds favors the production of fluorescent H_2 emission, requiring UV background intensity two orders of magnitude smaller than that measured in the Orion bar. We have presented evidence that this requirement is easily met in the central regions of NGC 3256.